Pure appl. geophys. 151 (1998) 1–16
0033–4553/98/010001–16 $ 1.50 + 0.20/0

Pure and Applied Geophysics

On the Elastic and Viscous Properties of Media Containing Strongly Interacting In-plane Cracks

T. DAHM[1] and TH. BECKER[1]

Abstract—We calculate elastic moduli and viscosities for media containing strongly interacting in-plane shear cracks. The cracks are randomly oriented or aligned, with equal length or a logarithmic size distribution. Our results from both a boundary element and a finite-element method suggest that the average moduli are best approximated by a differential, self-consistent model (DEM). Thus crack-to-crack interaction, which is considered in the DEM model, is important at high crack densities. This result seems to be different to results obtained from numerical experiments with highly fractured anti-plane shear cracks.

Key words: Cracks, cracked media, effective moduli.

1. Introduction

A medium containing numerous cracks behaves differently compared to the homogeneous medium. In seismology it is convenient to define average or effective elastic moduli to estimate the average elastic properties of the cracked medium.

O'CONNELL and BUDIANSKY (1974) have proposed a first model for the effect of nonintersecting cracks on the macroscopic elastic properties of solids based on a self-consistent approximation. However, the expressions that they arrived at for the dependence of the elastic constants of the material upon crack density appear unreasonable at high crack densities, since then their bulk and shear modulus become negative and their Poisson's ratio exceeds 0.5. Vanishing moduli at finite crack concentrations due to connecting cracks can be expected for real rocks near the percolation threshold and may be considered in an effective media model using additional constraints (e.g., MUKERJI *et al.*, 1995).

BRUNER (1976) and HENYEY and POMPHREY (1982) have modified the analysis of O'Connell and Budiansky and presented reasonable solutions for effective elastic constants always lying in the physical range. In our analysis we follow the method

[1] Institut für Meteorologie und Geophysik, Universität Frankfurt, Feldbergstr. 47, 60323 Frankfurt a. M., Germany. Fax: + +49 798 23280, Phone: + +49 798 28281, E-mail: dahm@geophysik.uni-frankfurt.de

of BRUNER (1976), which is sometimes called modified self-consistent approximation (e.g., DAVIS and KNOPOFF, 1995) or differential effective medium (DEM).

CHATTERJEE *et al.* (1978); HUDSON (1980); HUDSON and KNOPOFF (1989) showed that although the interaction between cracks is considered in the self-consistent model, the dipole-dipole interactions are neglected and may have a practical importance at high crack densities.

In order to investigate the importance of higher order crack-to-crack interaction, DAVIS and KNOPOFF (1995) numerically calculated the shear modulus of a solid body containing randomly oriented, strongly interacting, nonintersecting anti-plane cracks. Surprisingly, they found that a much simpler model (first-order perturbation theory, mean field model) than the self-consistent model, which totally neglects the crack-to-crack interaction, gives a more satisfactory approximation to the calculation of the effective shear modulus. At high crack concentrations and in the so-called long wavelength limit, the crack-to-crack interaction has a vanishing influence on the shear modulus and the *SH*-wave velocity.

Encouraged from the works of Davis and Knopoff, we performed numerical experiments with strongly interacting, nonintersecting in-plane shear cracks. The estimated shear modulus can for instance be used to predict the *SV*-wave velocity at high crack concentrations and in the long wavelength limit. Our results are inconsistent with the predictions of the mean field model. In contrast to DAVIS and KNOPOFF (1995) our elastic constants are more satisfactorily approximated by the DEM model, where crack-to-crack interaction is taken into account.

2. The Differential Effective Medium Model (DEM), Applied to In-plane Shear Cracks (2D)

The effect of interaction between cracks is induced by assuming that each crack behaves as embedded in a material having the average elastic properties of the cracked body. The approach of BRUNER (1976) is to consider a process whereby the crack density is gradually increased from zero to its final value. Let U be the strain energy per unit width of an equally deformed elastic body with area A under constant loading at its free boundaries (plane strain case, see HAHN, 1976, p. 180),

$$U = \frac{A}{4G_0}[(1-\nu_0)(\sigma_x+\sigma_y)^2 - 2(\sigma_x\sigma_y - \tau_{xy}^2)], \tag{1}$$

where G_0 and ν_0 are the shear modulus and the Poisson's ratio of the homogeneous, isotropic body, respectively, and σ_x, σ_y are the normal stresses in the x and y direction, respectively, and τ_{xy} is the shear stress. Inserting a single in-plane crack increases the total energy of the body by (e.g., HAHN, 1976, p. 132):

$$\Delta U = \frac{\pi a^2}{2G_0}(1 - \nu_0)\tau^2, \tag{2}$$

where a is the half-length of the crack and τ the shear traction on its surface before insertion. After insertion the shear traction on the crack is assumed to be zero.

2.1. Isotropic Case

The simplest model is to assume that the cracks are randomly oriented within the body, so that the overall elastic properties are still isotropic. Then, in the DEM approximation the rate of change of strain energy with respect to crack number n is equated by the same quantity as in (2), but expressed in terms of the applied constant load and the changing macroscopic elastic moduli of the isotropic, effective body.

$$\frac{dU}{dc} = \left[\frac{\partial U}{\partial G}\frac{dG}{dc} + \frac{\partial U}{\partial \nu}\frac{d\nu}{dc}\right] = \frac{dU}{dn}\frac{dn}{dc} \simeq \frac{A(1 - \nu(c))}{2G(c)}\langle\tau^2\rangle, \tag{3}$$

where

$$c = \frac{1}{A}\sum_{i=1}^{n}\pi a_i^2 = n\frac{\pi\langle a^2\rangle}{A}$$

is the crack density defined after DAVIS and KNOPOFF (1995), n is the number of cracks, and $\langle\tau^2\rangle$ is the mean of the squared shear tractions on the cracks. For randomly oriented cracks $\langle\tau^2\rangle$ is one half of the squared maximal shear stress in the body, $0.5 \cdot \tau_{\max}^2$. dU/dc in (3) is exact for randomly oriented cracks with equal length, and slightly overestimated for randomly oriented cracks with varying length.

Without loss of generality we choose the principal stresses σ_1 and σ_2 of the loading system inclined at 45° to the xy-coordinate system, so that

$$\sigma_x = \sigma_y = \frac{\sigma_1 + \sigma_2}{2}, \qquad \tau_{xy} = \tau_{\max} = -\frac{\sigma_1 - \sigma_2}{2}, \qquad \langle\tau^2\rangle = f \cdot \tau_{xy}^2,$$

where $f = 0.5$. This leads to

$$-[(1 - 2\nu)(\sigma_1 + \sigma_2)^2 + (\sigma_1 - \sigma_2)^2]\frac{1}{G}\frac{dG}{dc} - 2(\sigma_1 + \sigma_2)^2\frac{d\nu}{dc} = f(1 - \nu)(\sigma_1 - \sigma_2)^2. \tag{4}$$

This differential equation can be solved by choosing two different types of loading, e.g., pure shear ($\sigma_1 = -\sigma_2$) and uniform pressure ($\sigma_1 = \sigma_2$), which leads to

$$\nu(c) = \frac{(1 - \nu_0)\, e^{fc/2} + 2\nu_0 - 1}{2(1 - \nu_0)\, e^{fc/2} + 2\nu_0 - 1}$$

$$\frac{G(c)}{G_0} = \frac{1}{2(1 - \nu_0)\, e^{fc/2} + 2\nu_0 - 1}. \tag{5}$$

The effective Poisson's ratio $v(c)$ in (5) is limited between 0 and 0.5 and increases, while the effective shear modulus $G(c)$ decreases with increasing crack density (Fig. 1). A Poisson's ratio of $v_0 \approx 0.5$ is realized when the bulk modulus is much larger than the shear modulus. Replacing average strain by average strain rate $v_0 = 0.5$ can be viewed as an equivalent model to estimate effective viscosities.

2.2. Aligned Cracks

In the case that all cracks are inclined by an angle $\delta = 0°$ with respect to the maximal shear stress, the equation for the effective shear modulus in (5) can still be used when setting $f = 1$. We included this special case of aligned cracks in our numerical experiment for reasons given later.

We checked the validity of our assumption and give a brief explanation in the following. For a general anisotropic plane-strain case we can rewrite the stress strain relation for average stress and strain as:

$$\begin{pmatrix} \sigma_{xx} \\ \sigma_{yy} \\ \sigma_{xy} \end{pmatrix} = \begin{pmatrix} c_{xxxx} & c_{xxyy} & c_{xxxy} \\ c_{xxyy} & c_{yyyy} & c_{yyxy} \\ c_{xxxy} & c_{yyxy} & c_{xyxy} \end{pmatrix} \begin{pmatrix} e_{xx} \\ e_{yy} \\ e_{xy} \end{pmatrix},$$

where c_{ijkl} are components of the effective elasticity tensor, and $c_{ijkl} = c_{jikl} = c_{ijlk} = c_{klij}$ is valid. The six independent components of the elasticity tensor can in general be estimated by three experiments, e.g., simple shear (a) ($e_{xx} = e_{yy} = 0$, $e_{xy} = e$), pure shear (b) ($e_{xx} = -e_{yy} = e$, $e_{xy} = 0$), and uniform loading (c) ($e_{xx} = e_{yy} = e$, $e_{xy} = 0$). When all cracks are aligned and inclined with $\delta = 0°$ with respect to the x axis, the symmetry of the experiment and the symmetry of the single-crack deformation field ensure that the average components c_{xxxy} and c_{yyxy} are both zero. We proved this numerically for strongly interacting and randomly located but strictly aligned cracks.

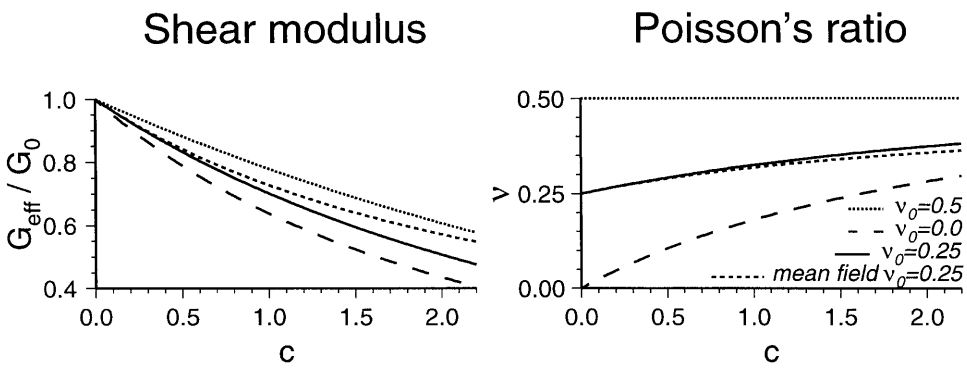

Figure 1
Relative effective shear modulus G_{eff}/G_0 and Poisson's ratio v as a function of the crack density c and different initial Poisson's ratios v_0. The predictions of the DEM model are plotted for $v_0 = 0$, 0.25 and 0.5, the ones of the mean field approximation for $v_0 = 0.25$.

A consequence of this special symmetry is that the average component c_{xyxy} is equal to the isotropic shear modulus G and can be estimated with a single simple shear experiment. We also numerically proved that uniform loading (c) and a pure shear experiment (b) generate no dislocation on the aligned cracks. In accord with theoretical expectations the shear forces on cracks are in both cases zero.

With these results it is easy to show that the average components fulfill, similar to the isotropic case, the relations $c_{xxxx} = c_{yyyy} = a + 2b$ and $c_{xxyy} = a$, where a and b are elastic constants. Therefore equations (1) and (4) with $f = 1$, originally derived for the isotropic case, can still be used to derive the effective elastic constants in (5).

However, we emphasize that average elastic properties are not isotropic for aligned cracks, it is only possible to compare one elastic constant estimated with a specific experiment with formulas derived for the isotropic case. We also recognize that our aligned-crack anisotropy problem is different from cracked (or layered) transverse isotropy problems addressed by others (e.g., ANDERSON *et al.*, 1974; HUDSON, 1980; PYRAK-NOLTE *et al.*, 1990). In our case we have six independent elastic constants (and two additional for anti-plane cracks) while the *SV*-wave propagation in transversely isotropic media is controlled by four elastic constants. However, our as well as transversely isotropic media allow purely transverse S waves propagating parallel or vertical to aligned cracks with a velocity of $v = (c_{xyxy}/\rho)^{1/2}$, where ρ is the rock density. We did not evolve the full dependence of velocity on incidence angle, which is beyond the scope of this paper.

3. Mean Field Approximation

In the mean field approximation one assumes that the rate of change of strain energy is independent of the crack concentration and equals (2), which leads to (HENYEY and POMPHREY, 1982; DAVIS and KNOPOFF, 1995):

$$v(c) = \frac{2v_0 + (1 - v_0)c}{2 + 2(1 - v_0)c}$$

$$\frac{G(c)}{G_0} = \frac{1}{1 + (1 - v_0)fc}. \tag{6}$$

Since crack-to-crack interactions are neglected in the mean field model, the change in elastic constants with respect to crack density is smaller than predicted from the DEM model (Fig. 1).

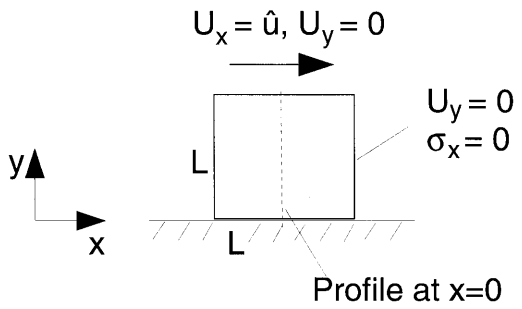

Figure 2
Geometry and boundary conditions of the numerical experiment. The body is subjected to a constant dislocation in x direction at its top and fixed at the bottom. The side walls are free of normal stress and fixed in y direction.

4. Numerical Experiments

We simulate a simple shear experiment to estimate the effective shear modulus. A quadratic elastic body with side length L is fixed at its bottom and sheared at its upper boundary with a constant displacement $u_x = \hat{u}$ (Fig. 2). Movement on the side walls is restricted in the horizontal direction. Due to the defined deformation, the shear stress τ_{xy} within the body takes a final value, from which the effective shear modulus can be estimated by:

$$G_{\text{eff}} = \frac{\langle \tau_{xy} \rangle}{2\langle e_{xy} \rangle} = \langle \tau_{xy} \rangle \frac{L}{\hat{u}}, \tag{7}$$

where $\langle e_{xy} \rangle = \hat{u}/2L$ is the average shear deformation, and $\langle \tau_{xy} \rangle$ the average shear stress within the body. The relative effective shear modulus is calculated from the shear stress of the homogeneous body (τ_0) and the average shear stress of the cracked body under the same boundary conditions by:

$$\frac{G_{\text{eff}}}{G_0} = \frac{\langle \tau_{xy} \rangle}{\tau_0}. \tag{8}$$

DAVIS and KNOPOFF (1995) estimated effective shear moduli from the energy of the composite. In our experiment the energy of the composite depends not only on the shear modulus, but also on the Poisson's ratio. Therefore we chose eq. (8) to estimate G_{eff}. We used a boundary element method of CROUCH and STARFIELD (1983) and a modified finite-element method of ZIENKIEWICZ (1977) to model the elastic behavior of the cracked body.

4.1. Boundary Element Method

In the boundary element method (BEM) the cracks within the body are divided into straight line segments on which the magnitudes of constant dislocations are treated as unknowns that are solved for by satisfying stress-free boundary conditions at the center of the line segment. The interaction between cracks is taken into consideration using analytic kernel functions of homogeneous media. The boundaries of the body itself are simulated by placing fictitious dislocation sources on it and demanding the stress or displacement on the inner side to be zero. This is a correct approach as long as the body is completely surrounded by fictitious dislocation sources.

The stresses and displacements at an arbitrary point within the body are calculated in a second step from the dislocations on the cracks and boundaries of the body.

The calculated magnitudes of crack and boundary dislocation sources are accurate when enough line segments are used to sample the problem. As a rule of thumb one must carefully consider that the minimal distance between neighboring cracks is slightly larger than the length of the line segments on the cracks. For example, we divided each crack into segments of equal length (between 2 and 36 segments, depending on the length of the crack), and fixed the minimal distance between cracks to more than one and a half segment lengths.

DAVIS and KNOPOFF (1995), who also used a boundary element method, simulated up to 10000 cracks with up to 64 line segments. To solve such large inversion problems they used a Jacobi iterative scheme, and had to choose initial values of displacements to be those of the noninteracting case. We find that our smaller simulations (between 100 and 160 cracks) are large enough to face the problem of crack interaction, and we were able to use a standard inversion routine like LU factorization to solve the inversion problem within a reasonable time (several minutes to hours).

4.2. Finite Elements

The finite-element method (FE) used is an implementation of the split-node technique as introduced by MELOSH and RAEFSKY (1981). It modifies the standard set of equations' force vector (see e.g., ZIENKIEWICZ, 1977, for a description of the FE method) to enable the incorporation of dislocations at special nodes in a discrete grid. Prescribing the slip distribution along embedded lines of nodes, one is able to model the elastic media's response to cracks or faults. The boundary value problem of stress-free crack surfaces under external loading was iteratively solved. In the first step an initial slip on each crack-node was applied such that the shear stress is reduced. After calculating the inverse coefficient matrix once and solving for the resulting stress field, the remaining shear stress on each crack-node was used

to estimate an incremental slip added in the next iteration. The iteration process was terminated when the remaining stress on each crack-node dropped below 10^{-4} of the loading stress. Generally 200 iterations within 10 to 20 minutes CPU-time were needed to simulate single crack problems.

The FE single crack solution accurately converged to the analytical solution when enough crack-nodes were introduced. Using a typical crack-node interval of $\Delta x \approx 0.04 \times a$, where a is the half-length of the crack, resulted in a deviation of the estimated to the theoretical slip of about 2%.

We chose linear form functions and triangular elements. All meshes have been generated automatically using a gridding routine of SHEWCHUK (1996). The nodal distribution was constrained to be equidistant on the cracks, to show a higher density on the crack tips and to obey a minimum angle of 25° and maximum area of $a^2/16$ at each element. The maximum number of nodes used was 18000.

4.3. *Accuracy of our Calculations*

We compared the numerical solutions with analytical solutions for the single crack under pressure and under shear (e.g., POLLARD and SEGALL, 1989) and found satisfactory agreement for both the boundary element method as well as the finite-element method (Fig. 3). For strongly interacting cracks analytical solutions are not available. We cross-checked the results obtained with both methods. Figure 4 gives an example of the estimated shear stress over a profile at $x = 0$ (see Fig. 2) that crosses several systematicallly aligned cracks ($\delta = 0°$, $c = 1.6$). The shear stress approaches zero at the crack crossing points. The small differences in estimated shear stress are due to different fine sampling of the boundary value problem.

Average shear stress was calculated from the estimated shear stress within the body. For the boundary element analysis we thereby excluded stress estimates at

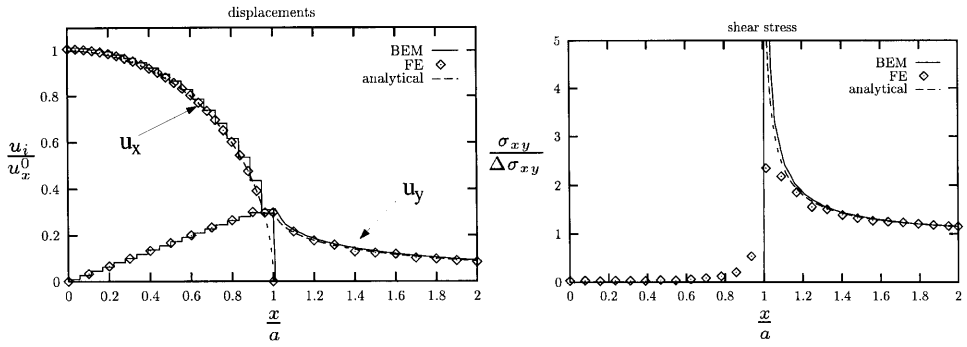

Figure 3
Comparison of the analytical and numerical single crack solution (left: displacements u_x and u_y; right; shear stresses σ_{xy}) on a profile on the x axis. The stress-free in-plane shear crack under constant shear load $\Delta\sigma_{xy}$ was placed on $y = 0$ between $x = \pm a$.

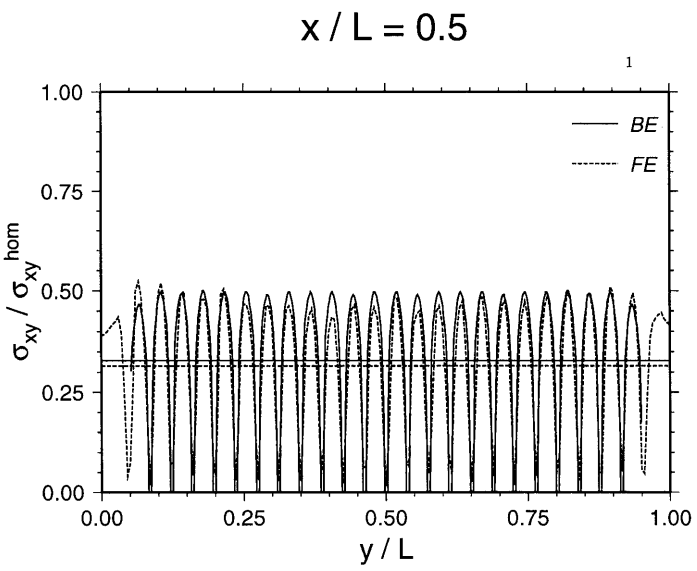

Figure 4
The normalized shear stress and its average as estimated with the boundary element (BE) and finite-element method (FE) versus the distance y/L along a profile at $x = 0$.

points near the boundary and the corner of the composite, where the segment length of the sampled boundary became important. The estimated average stress in Figure 4 from both methods differs about 1%.

5. Results

Different types of crack distributions have been modelled. First we used randomly oriented cracks of equal length and of a logarithmic length distribution (Fig. 5),

$$l = 2a(j) = 2^j \cdot \frac{L}{100},$$

with $j = 0, 1, \ldots, 5$ and $n(j) = \text{INT}\{(6 - j) \cdot \text{NMAX}/21\}$. Either the length of the cracks ($2a$) or the total number of line segments (NMAX) was varied between 900 and 2000 to create crack densities between $c = 0.87$ and $c = 2.0$. The maximum number of cracks was about 160. For randomly oriented cracks of equal length we had the problem that at crack densities larger than $c = 1$ the ordering within subregions steadily increased when rejecting the random choice of a crack that intersect with another one. As a consequence the cracks were not really randomly oriented, and $f = 0.5$ was not always met at large crack densities. To minimize

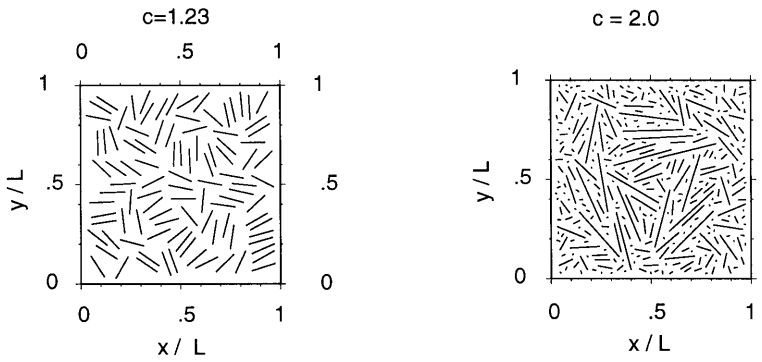

Figure 5
Randomly oriented cracks of equal length (left) and of a logarithmic length distribution (right) with crack densities of $c = 1.23$ and $c = 2.0$, respectively.

effects of a discrete crack distribution we averaged effective moduli from different distributions with identical crack density.

These problems are avoided with aligned cracks, which is a second class of models we tested. We simulated systematically aligned cracks of equal length, and randomly distributed but equally oriented cracks of equal length and of a logarithmic length distribution (Fig. 6). About 100 cracks were used and the length of the cracks was increased to increase the crack density from $c = 0$ to about 2. Usually six to ten line segments have been chosen per crack. The effective shear modulus as a function of the crack density and the Poisson's ratio is, for both randomly oriented (Fig. 7) and aligned cracks (Fig. 8), best approximated with the DEM model.

Effective moduli calculated with the FE method are systematically larger than the ones from the BEM method (Fig. 8). A closer look at this revealed that the differences are due to a rough discretization in the corners of the FE models. This introduces an artificial stiffness in the corners of the model, resulting in larger effective shear moduli. Generating finer FE grids is in principle possible, but would at this time exceed the core memory and CPU time available to us.

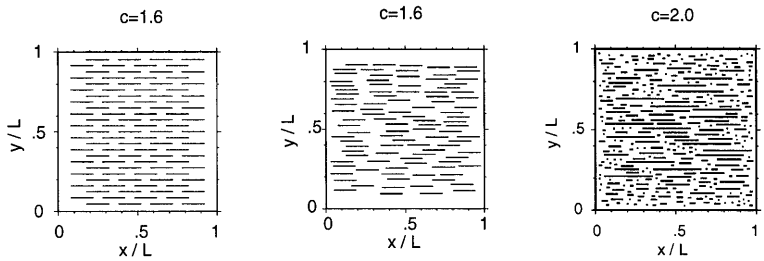

Figure 6
Systematic aligned cracks (left), randomly aligned cracks of equal length (middle) and of a logarithmic length distribution (right). The crack density is $c = 1.6$, 1.6 and 2.0, respectively.

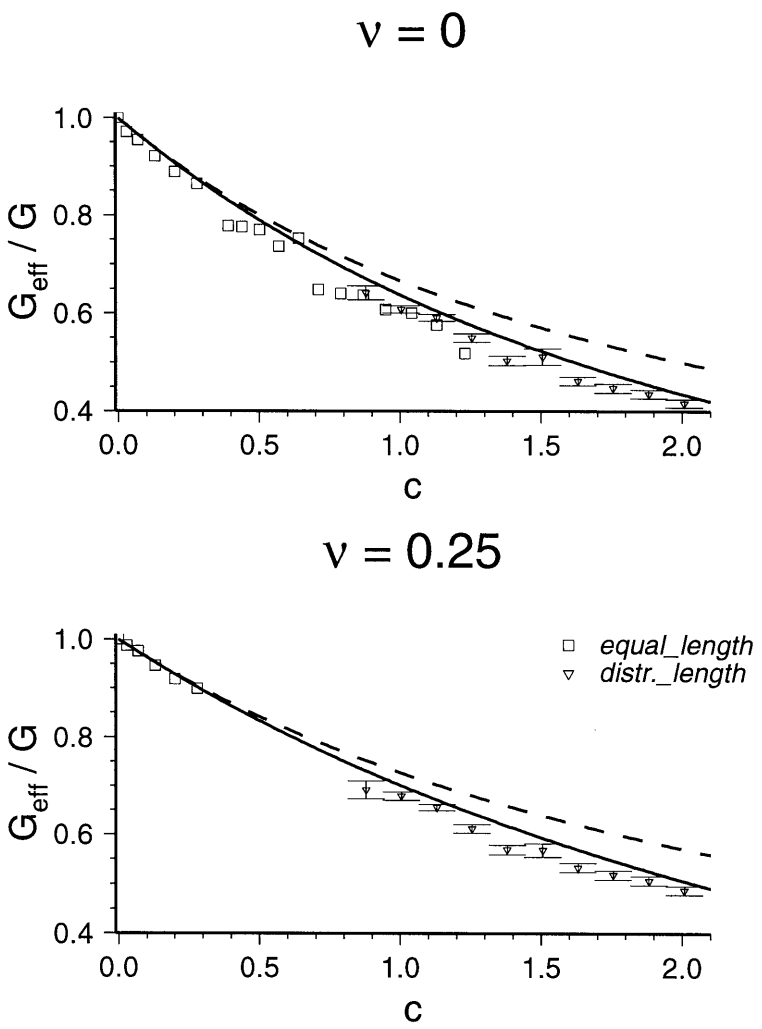

Figure 7
Shear modulus with respect to crack density for randomly oriented cracks of equal length and of a logarithmic length distribution. The soid line shows the DEM solution, and the dashed line the mean field solution.

The results obtained for effective shear moduli under matrix Poisson's ratios of 0.5 can be transferred to estimate the effective viscosities of fractured or foliated viscoelastic media (Fig. 9). Using the vicoelastic correspondence principle (e.g., CHRISTENSEN, 1982) it is possible to show that stress-free cracks under short-term constant shear and long-term constant shear rate behave identically when substituting the shear modulus through viscosity. We explicitly proved this by extending and applying the boundary element program to viscoelastic crack problems.

The essential assumption in the viscoelastic model is that the crack density, e.g., within a fault zone, remains constant over a long enough time. In this model individual cracks or faults may heal and others may be newly generated.

6. Discussion

This 2D study is restricted to highly fractured in-plane shear cracks, with the hope that some broad generalizations can be elucidated that will help in the solution of problems involving more complicated geometries. We have not investigated the problem of a medium near the percolation threshold, where through-going fractures and vanishing of the shear modulus will take place.

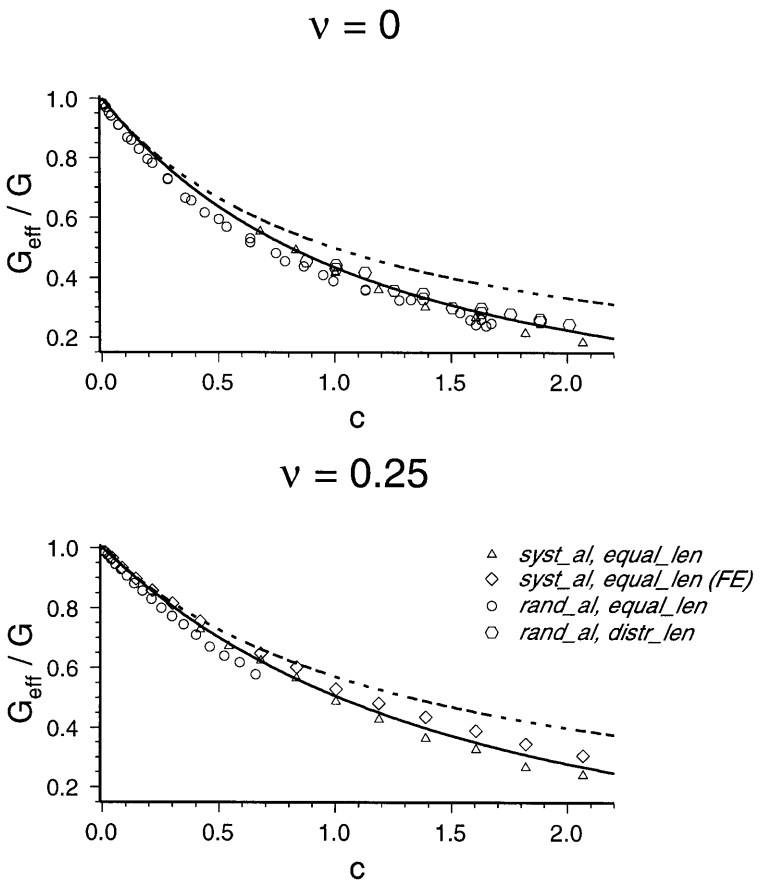

Figure 8
Shear modulus with respect to crack density for aligned cracks. See Figure 7 for further explanations.

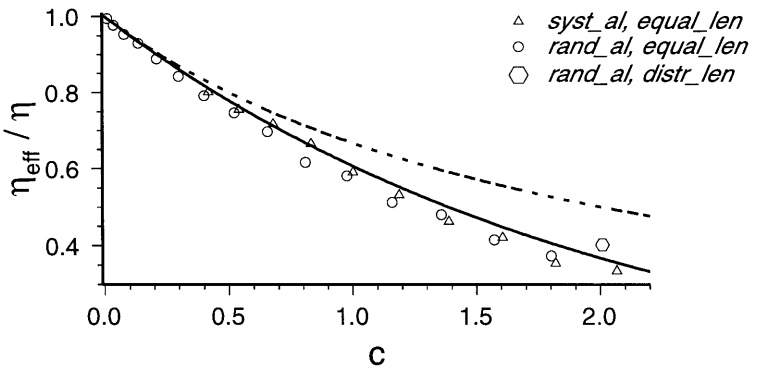

Figure 9
Effective viscosity with respect to crack density for aligned cracks.

The good consistency of our numerically estimated effective shear moduli and the predictions of the DEM model at high crack densities is plausible and not unexpected. The DEM model considers crack-to-crack interaction which is increasingly important with decreasing distance to neighboring cracks.

However, surprise is the different character of our solution for in-plane cracks (mode II) to comparable studies of anti-plane cracks (mode III). DAVIS and KNOPOFF (1995) found that for highly fractured anti-plane cracks the crack-to-crack interaction can be neglected when predicting effective moduli. As suggested by their numerical studies they proposed a theory for the interaction of anti-plane cracks, which unfortunately is not applicable to in-plane cracks.

To better understand these different results we looked at differences in analytical solutions between mode II and III shear cracks. The crack-tip singularity, the most pronounced stress perturbation in the near field of a crack, may play an important role for the interaction between cracks. The decrease of stress away from the tip singularity is for both mode II and III cracks proportional to the reciprocal square-root over the distance. Also the strength of the mode II and III singularity, measured by the stress intensity factor K, is of equal size for single as well as periodic collinear cracks. Analytic solutions of periodic collinear cracks are of special interest since their crack-to-crack interaction leads to a steady increase of K-values with decreasing distance between the cracks (Fig. 10, and GROSS, 1996). For collinear periodic cracks, interaction near the tip is of equal importance for both mode II and III cracks. The strong and evenly enhanced stress singularity of interacting cracks has not been considered in the theory proposed by DAVIS and KNOPOFF (1995), since they neglect the contribution to the perturbation stress field from regions between narrowly spaced crack-tips.

Both, the equal strength and radial attenuation of the stress singularity at the crack tip indicates that the influence of one crack to another is similar for mode II and III cracks.

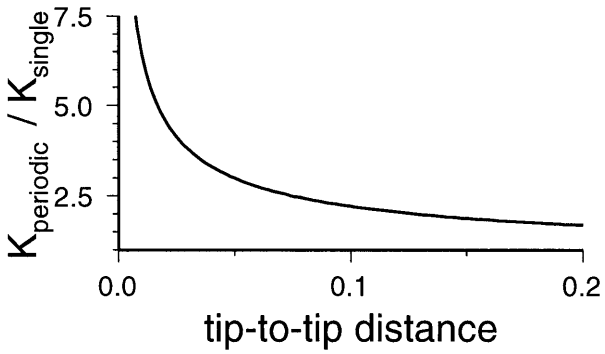

Figure 10
Amplification factor of the strength of the crack tip singularity versus the tip-to-tip distance (normalized to the crack length) for collinear periodic mode II and III cracks (e.g., GROSS, 1996).

Another measure of the interaction potential is given by the spatial pattern of the perturbation strain energy. Neighboring cracks within regions of enhanced perturbation strain energy behave differently compared to homogeneous loading. The perturbation strain energy of mode II cracks has four major lobes, two in crack-direction and two orthogonal to the crack, while that of a mode III crack has

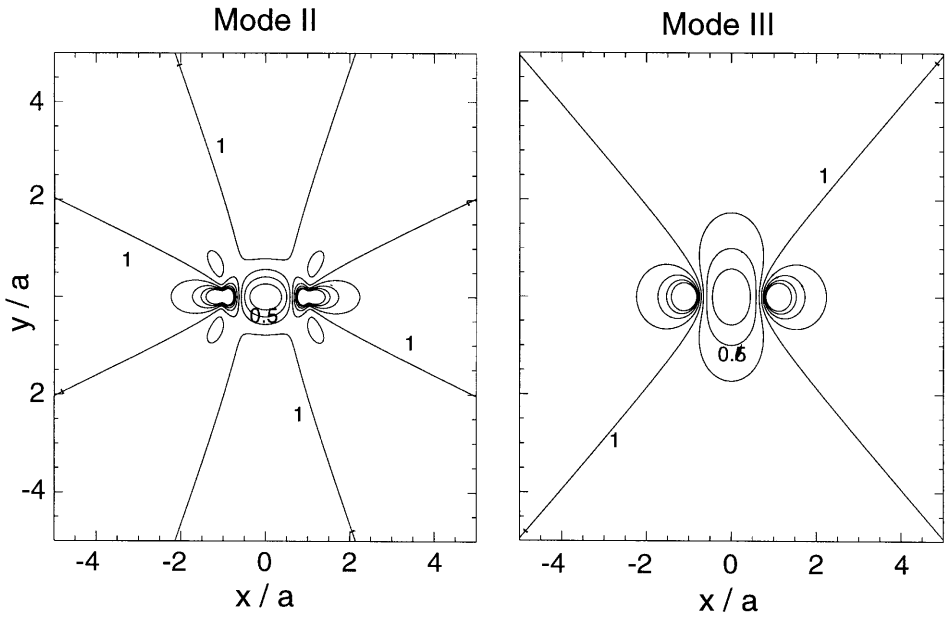

Figure 11
Perturbation strain-energy $\times 2G$ for a mode II and a mode III crack. The crack with half-length a is placed on the x axis between $-1 \leq x/a \leq 1$.

only two lobes in crack-direction (Fig. 11, and POLLARD and SEGALL, 1989). On a profile at $y = 0$ both modes generate the same strain energy for $|x| > a$, while on a profile at $x = 0$ the mode II strain energy is larger than that of mode III crack. This different pattern may influence the interaction between cracks. However, this comparison does not suggest that crack-to-crack interaction can be totally neglected for mode III cracks and is important for mode II cracks.

7. Summary

The differential effective self-consistent model gives the best approximation to predict the moduli of media with strongly interacting in-plane cracks. This seems to be different for strongly interacting anti-plane cracks, for which a model disregarding the crack-to-crack interaction gives better approximations. We transferred our results to predict effective viscosities, which may be considered to estimate the long-term behavior of foliated regions or of fractured viscoelastic media with steady-state crack densities.

Acknowledgements

We thank Heiner Igel for bringing the subject of highly fractured media to our mind, and for discussion throughout the work. Harro Schmeling and Gerhard Müller improved the manuscript through their suggestions and interest. We also thank Prof. Hui Zhu Yang and another anonymous reviewer for their comments and suggestions.

REFERENCES

ANDERSON, A., MINSTER, B., and COLE, D. (1974), *The Effect of Oriented Cracks on Seismic Velocities*, J. Geophys. Res. *79*, 4011–4014.

BRUNER, W. (1976), *Comment on "Seismic Velocities in Dry and Saturated Cracked Solids" by Richard J. O'Connell and Bernard Budiansky*, J. Geophys. Res. *81*, 2573–2576.

CHATTERJEE, A., MAL, A., and KNOPOFF, L. (1978), *Elastic Moduli of a Cracked Solid*, J. Geophys. Res. *83*, 1785–1792.

CHRISTENSEN, R., *Theory of Viscoelasticity* (Academic Press, New York 1982).

CROUCH, S., and STARFIELD, A., *Boundary Element Methods in Solid Mechanics* (George Allan and Unwin, London 1983).

DAVIS, P., and KNOPOFF, L. (1995), *The Elastic Modulus of Media Containing Strongly Interacting Antiplane Cracks*, J. Geophys. Res. *100*, 18253–18258.

GROSS, D., *Bruchmechanik* (Springer, Berlin 1996).

HAHN, H., *Bruchmechanik* (B. G. Teubner, Stuttgart 1976).

HENYEY, F., and POMPHREY, N. (1982), *Self-consistent Elastic Moduli of a Cracked Solid*, Geophys. Res. Lett. *9*, 903–906.

HUDSON, J. (1980), *Overall Properties of Cracked Solid*, Math. Proc. Cambridge Philos. Soc. *88*, 371–384.

HUDSON, J., and KNOPOFF, L. (1989), *Predicting the Overall Properties of Composites—Material with Small-scale Inclusions or Cracks*, Pure appl. geophys. *131*, 551–576.

MELOSH, H., and RAEFSKY, A. (1981), *A Simple and Efficient Method for Introducing Faults into Finite Element Computations*, Bull. Seismol. Soc. Am. *71*, 1391–1400.

MUKERJI, T., BERRYMAN, J., MAVKO, G., and BERGE, P. (1995), *Differential Effective Medium Modeling of Rock Elastic Moduli with Critical Porosity Constraints*, Geophys. Res. Lett. *22*, 555–558.

O'CONNELL, R., and BUDIANSKY, B. (1974), *Seismic Velocities in Dry and Saturated Cracked Solids*, J. Geophys. Res. *79*, 5412–5426.

POLLARD, D., and SEGALL, P., *Theoretical displacements and stresses near fractures in rock: with application to faults*, *joints*, *veins*, *dikes*, *and solution surfaces*. In *Fracture Mechanics of Rocks* (Aktinson, B., ed.) (Academic Press, Inc., San Diego 1989) pp. 277–347.

PYRAK-NOLTE, L. J., MYER, L. R., and COOK, N. G. W. (1990), *Anisotropy in Seismic Velocities and Amplitudes from Multiple Parallel Fractures*, J. Geophys. Res. *95*, 11345–11358.

SHEWCHUK, J. (1996), *Triangle: Engineering a 2D quality mesh generator and Delaunay triangulator*. In *First Workshop on Applied Computational Geometry*. Association for Computing Machinery, pp. 124–133.

ZIENKIEWICZ, O., *The Finite Element Method* (McGraw-Hill Book Company, London 1977) 3rd edition.

(Received March 29, 1997, accepted May 31, 1997)

.